arXiv:1402.2989v2 [cond-mat.mes-hall] 14 Feb 2014

# The $\nu = 5/2$ Fractional Quantum Hall State in the Presence of Alloy Disorder

Nianpei Deng[1], G.C. Gardner[2,3], S. Mondal[1,2], E. Kleinbaum[1], M.J. Manfra[1,2,3,4], and G.A. Csáthy[1,2]
[1] *Department of Physics, Purdue University, West Lafayette, IN 47907, USA*
[2] *Birck Nanotechnology Center, Purdue University, West Lafayette, IN 47907, USA*
[3] *School of Materials Engineering, Purdue University, West Lafayette, IN 47907, USA*
[4] *School of Electrical and Computer Engineering, Purdue University, West Lafayette, IN 47907, USA*

(Dated: February 17, 2014)

We report quantitative measurements of the impact of alloy disorder on the $\nu = 5/2$ fractional quantum Hall state. Alloy disorder is controlled by the aluminum content $x$ in the $Al_xGa_{1-x}As$ channel of a quantum well. We find that the $\nu = 5/2$ state is suppressed with alloy scattering. To our surprise, in samples with alloy disorder the $\nu = 5/2$ state appears at significantly reduced mobilities when compared to samples in which alloy disorder is not the dominant scattering mechanism. Our results highlight the distinct roles of the different types of disorder present in these samples, such as the short-range alloy and the long-range Coulomb disorder.

Unraveling the impact of disorder is an important endeavor in contemporary condensed matter physics. Disorder is well understood in the single particle regime. Examples of fundamental importance are Anderson localization [1] and universal plateau-to-plateau transition in the integer quantum Hall effect [2]. Localization in the presence of the disorder is also important in topological insulators [3] and in atomic condensates [4]. In contrast, understanding disorder in correlated electron systems continues to pose serious challenges. The interplay of disorder and interactions has witnessed renewed interest in the two-dimensional electron gas (2DEG) in connection to the stability of the exotic fractional quantum Hall states (FQHS) [5–7] and in graphene due to the observation of a wealth of FQHSs using local detection [8].

The FQHS at Landau level filling factor $\nu = 5/2$ is one example of a correlated ground state which has attracted considerable attention [10–27]. This is because of the putative exotic Pfaffian-like correlation in the ground state at $\nu = 5/2$ and of the non-Abelian quasiparticle excitations [28–30]. Non-Abelian quasiparticles may be used to realize topological qubits, building blocks of fault-tolerant quantum computers [31]. Furthermore, since the Pfaffian can be mapped into a paired wavefunction with a $p$-wave symmetry [28, 29, 32], the $\nu = 5/2$ FQHS is intimately connected to $p$-wave superconductors [33], Majorana physics in superconductor-semiconductor hybrid devices [34], and superfluid $^3$He [35].

The effect of the disorder on the $\nu = 5/2$ FQHS remains largely unknown [5–7]. Disorder is a key factor in limiting $\Delta_{5/2}$, the energy gap of the $\nu = 5/2$ FQHS, to less than 0.6 K [14, 15, 17]. Measurements of this state must therefore be conducted at either dilution or nuclear demagnetization refrigerator temperatures, which render these studies time consuming [11, 36]. However, in the disorder-free limit $\Delta_{5/2}$ is predicted to be as high as 2 K at the typical electron density of $n = 3 \times 10^{11}/\text{cm}^2$ [37–41]. Understanding disorder in the $\nu = 5/2$ FQHS is thus expected to lead to an increased energy gap with the following benefits toward fundamental tests of the nature of this state: a) experiments may be conducted at higher temperatures, possibly in $^3$He refrigerators, with shorter turn-around times allowing for extensive investigations b) improved signal-to-noise ratio in experiments on nanostructures in which the edge states of the $\nu = 5/2$ FQHS are probed [23–26] and c) exponentially enhanced topological protection in qubits [31].

Studies of disorder require the capability of its control. In this Letter we report on a quantitative inquiry of the impact of a specific type of short-ranged disorder, alloy disorder, on the $\nu = 5/2$ FQHS. We investigated a series of specially engineered samples in which all parameters but the alloy disorder remain constant by design [42]. Specifically, we measured $Al_{0.24}Ga_{0.76}As/Al_xGa_{1-x}As/Al_{0.24}Ga_{0.76}As$ quantum wells in which the electrons are confined to the $Al_xGa_{1-x}As$ alloy and which have different values of the aluminum molar fraction $x$ [42]. Since the disorder is added to the electron channel during the Molecular Beam Epitaxy (MBE) growth, it is controlled and precisely quantified. Disorder is found to suppress the energy gap of the $\nu = 5/2$ FQHS. However, to our surprise we find strong $\nu = 5/2$ FQHSs in alloy samples at values of the electron mobility at which this state does not develop at all in the highest quality alloy-free samples. The mobility threshold for the formation of the $\nu = 5/2$ FQHS in the alloy samples is thus much reduced as compared to that in the alloy-free samples. Our results indicate that the engineering of the exotic FQHSs, such as the one at $\nu = 5/2$, is critically dependent on the different length scales of competing disorders present in the 2DEG: the

short-range alloy and interface roughness disorder and the long-range Coulomb disorder.

A sketch of the active region of our alloy-free reference sample and of a sample containing alloy disorder are shown in the insets of Fig.1. The sample growth procedure and characterization of our samples at $T = 300$ mK can be found in Ref.[42]. Details of the samples, of the state preparation, and of other aspects of the low temperature measurements reported in this Letter can be found in the Supplementary Materials section. We note that MBE-controlled alloy disorder was first introduced to 2DEGs in Ref.[43]. However, in these samples [2, 43, 44] the $\nu = 5/2$ FQHS has not been observed. In contrast, our samples have several essential features which are optimized for a strong $\nu = 5/2$ FQHS even in the presence of the disorder. First, the 2DEG is confined to a symmetrically doped quantum well rather than a single heterointerface. This allows for a higher electron density, enhancing therefore fragile FQHSs. Second, we use a reduced Al content 0.24 in the $Al_{0.24}Ga_{0.76}As$ barriers, which enhances the $\nu = 5/2$ FQHS [7, 13, 46]. Third, we use a short period superlattice doping scheme [45], which is known to yield a strong $\nu = 5/2$ FQHS [5, 46, 47].

It is important to appreciate that only the alloy disorder is different in each sample. All other sample parameters, however, are left virtually unchanged. In order to avoid any density dependent effects the electron density is kept constant, close to $n \simeq 2.9\times10^{11}/\mathrm{cm}^2$. Specifically, in our samples $2.70 \times 10^{11}/\mathrm{cm}^2 \leq n \leq 3.08 \times 10^{11}/\mathrm{cm}^2$. Furthermore, the alloy content $x$ of the electron channel $Al_xGa_{1-x}As$ is low when compared to that in the confining $Al_{0.24}Ga_{0.76}As$. There is therefore virtually no variation of the electronic effective mass $m$ and of the electronic confinement in the direction perpendicular to the plane of the 2DEG [48]. Other parameters held constant include the position of the 2DEG relative to the sample surface and the thickness of the capping layer [49].

Fig.1 shows the magnetoresistance $R_{xx}$ and the Hall resistance $R_{xy}$ of the alloy-free reference sample, i.e. for which $x = 0$, measured at $T = 7$ mK in a van der Pauw geometry. The figure is limited to magnetic fields $B$ for which the filling factor ranges between $2 < \nu < 3$, commonly referred to as the lower spin branch of the second Landau level. Because of the high quality growth and sample design described earlier we observe strong FQHSs at $\nu = 5/2$, $2 + 1/3$, and $2 + 2/3$ as indicated by vanishing $R_{xx}$ and quantized $R_{xy}$ [10, 50]. Other more fragile FQHSs are also seen in Fig.1 [12, 17].

Alloy disorder strongly affects magnetoresistance. This can be seen in the traces of the sample with $x = 0.0036$ gathered at 7 mK, which are also shown in Fig.1. The most fragile FQHSs, such as the $\nu = 2+2/5$, $2+1/5$, and $2 + 4/5$ FQHSs, are destroyed. The FQHS at $\nu = 5/2$, however, remains fully quantized in spite of the presence of alloy disorder. Indeed, at this $\nu$ there is a vanishing

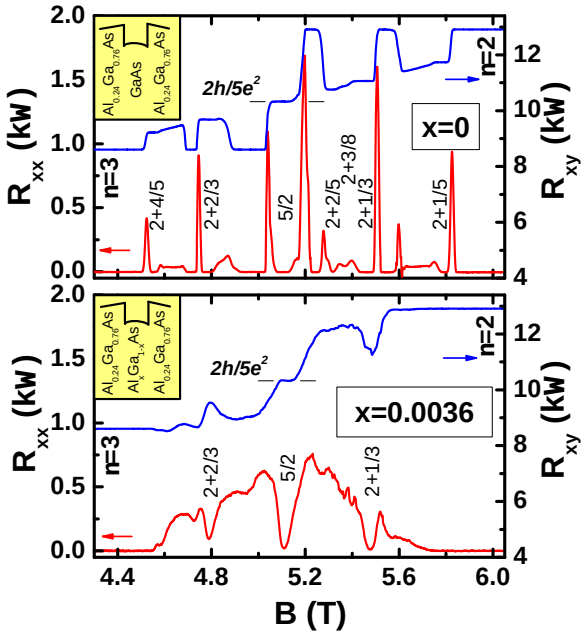


FIG. 1. Magnetoresistance $R_{xx}$ and Hall resistance $R_{xy}$ in the reference sample with $x = 0$ (top panel) and the alloy sample with $x = 0.0036$ (bottom panel) as measured at 7 mK. Numbers indicate the filling factors of various FQHSs and insets are sketches of the sample structure.

$R_{xx}$ and the rigorously quantized $R_{xy} = 2h/5e^2$, which holds to a precision of 1 part in $10^3$.

Next we have investigated the temperature dependence of the $\nu = 5/2$ FQHS. Thermalization of electrons in our experiment is assured by the use of a $^3$He immersion cell [11, 51] and temperature measurements of the $^3$He bath below 100 mK are performed with the aid of a tuning fork viscosity thermometer [51]. At the lowest temperatures $T$ the magnetoresistance of the $\nu = 5/2$ FQHS follows an activated form $R_{xx} \propto \exp(-\Delta_{5/2}/2T)$, from which we extract the energy gap $\Delta_{5/2}$. The inset of Fig.2 shows the temperature dependence of $R_{xx}$ at $\nu = 5/2$ on an Arrhenius plot, i.e. $\ln R_{xx}$ as function of $1/T$. The presence of the linear segment indicates that transport is activated. In the alloy-free reference sample we find a record high energy gap $\Delta_{5/2} = 569$ mK [17].

The inset of Fig.2 also shows the $T$-dependence of $R_{xx}$ at $\nu = 5/2$ in two representative alloy samples with $x = 0.00075$ and $x = 0.0036$. The presence of linear segments at non-zero $x$ means the survival of activated transport even in the presence of alloy disorder. It is, therefore, meaningful to extract energy gaps in the alloy samples as well. Values found are tabulated in the Supplementary Materials section and are plotted as function of $x$ in Fig.2. We find the $\Delta_{5/2}$ has a decreasing trend with an increasing $x$. At the largest value of $x = 0.0046$ we studied, we no longer observe a FQHS at $\nu = 5/2$. A

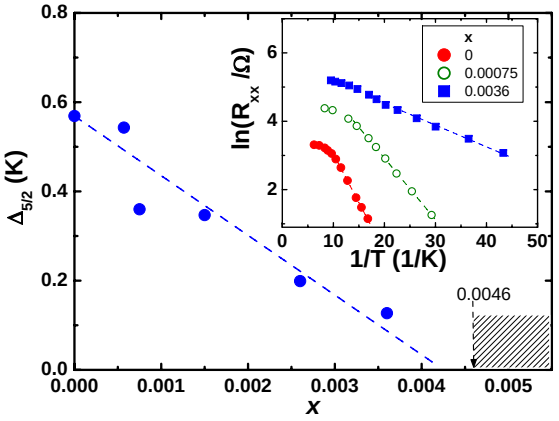


FIG. 2. The dependence of $\Delta_{5/2}$ on the aluminum mole fraction $x$. In a sample with $x = 0.0046$ we do not observe a FQHS at $\nu = 5/2$, hence the excluded shaded area. The inset shows Arrhenius plots for the $\nu = 5/2$ FQHS in three representative samples.

linear fit to the data passing through the point associated with the $x = 0$ reference sample shows that the gap closes at the extrapolated value of $x \simeq 0.0042$. We note that the error in $\Delta_{5/2}$ as determined from the Arrhenius fits is estimated to $\pm 10\%$. However, in Fig.2 there is also scatter in the data possibly caused by small variations in the sample densities and slight variations from the target value of the alloy content $x$.

The aluminum fraction $x$ in our alloy samples is clearly a measure of the added disorder. In the literature the most commonly used metric for the disorder is the mobility $\mu$. Early work on the $\nu = 5/2$ FQHS found that the energy gap of the state correlates well with the mobility [14]. It was found that a higher $\mu$ resulted in a larger $\Delta_{5/2}$ and the $\nu = 5/2$ FQHS does not develop for mobility less than the threshold value $\mu_C \simeq 10 \times 10^6 \mathrm{cm}^2/\mathrm{Vs}$. Later it became apparent that there is in fact a poor correlation between $\Delta_{5/2}$ and $\mu$ [7, 16]. Nonetheless, a threshold $\mu_C$ below which a $\nu = 5/2$ FQHS does not develop was still identified. The shaded area of Fig.3 shows the stability region of the $\nu = 5/2$ FQHS in high quality alloy-free samples at densities $2.65 \times 10^{11} \leq n \leq 3.2 \times 10^{11}/\mathrm{cm}^2$ close to that of our samples [6, 7, 13–17]. These data are taken from the literature. A threshold value $\mu_C \simeq 7 \times 10^6 \mathrm{cm}^2/\mathrm{Vs}$ for these alloy-free samples is clearly seen.

Fig.3 also shows that a strong $\nu = 5/2$ FQHS with $\Delta_{5/2} = 127$ mK develops in the alloy sample with $\mu = 2.2 \times 10^6 \mathrm{cm}^2/\mathrm{Vs}$. This is surprising, since at such a low mobility a $\nu = 5/2$ FQHS has never been observed. Indeed, this mobility is much below the the previously established $\mu_C \simeq 7 \times 10^6 \mathrm{cm}^2/\mathrm{Vs}$ threshold in high quality alloy-free samples. We thus found that the mobility threshold for a fully quantized $\nu = 5/2$ FQHS is significantly lowered in the presence of alloy disorder and, therefore, the $\nu = 5/2$ FQHS is robust to the presence of alloy disorder. Furthermore, we conclude that alloy disorder does not appear to be as detrimental to the development of the $\nu = 5/2$ FQHS as the residual disorder unintentionally added during sample growth. The gap $\Delta_{5/2}$ for our alloy samples closes at an extrapolated new threshold of $\mu_C^{alloy} \simeq 1.8 \times 10^6 \mathrm{cm}^2/\mathrm{Vs}$.

It is important to appreciate that not only our samples have controllably added alloy disorder but, with the exception of the sample with $x = 0.00057$, alloy disorder is the dominant scattering mechanism. This is the case because the electron scattering rate in our alloy samples $1/\tau$ exceeds the residual scattering rate of the alloy-free reference sample $1/\tau_{residual} = 1.3\mathrm{ns}^{-1}$ [42]. Here $\tau = \mu m/e$ is the transport scattering time. As seen in Fig.3, $\Delta_{5/2}$ is linearly decreasing with $1/\tau$ with the slope of 41 mK·ns. Furthermore, we find that the gap extrapolates to zero near $1/\tau \simeq 15$ ns$^{-1}$.

Since Al is a neutral impurity, when added to a perfect GaAs crystal, it perturbs the crystal potential on sub-nanometer length scale. The alloy disorder we study thus generates a short-range scattering potential [43]. In a recent experiment a different type of short-range disorder, that due to surface roughness scattering, was investigated [6]. It was found that in a heterojunction insulated gate field-effect transistor $\Delta_{5/2}$ increases with a decreasing mobility, a result which is opposite to our findings. One reason for this discrepancy is that in Ref.[6] the electron density is increased as the mobility is decreasing. The quantitative effect of the disorder on the energy gap

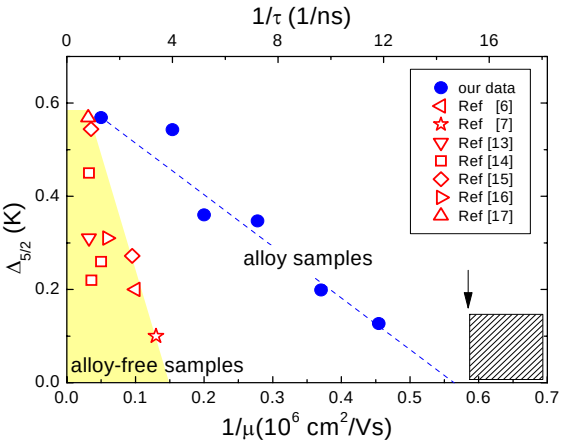


FIG. 3. The dependence of $\Delta_{5/2}$ on inverse mobility $1/\mu$ and the electronic scattering rate $1/\tau$ of our samples (closed symbols) and of alloy-free samples from the literature with densities near $2.9 \times 10^{11}/\mathrm{cm}^2$. In our alloy samples the $\nu = 5/2$ FQHS survives at surprisingly high $1/\mu$ and, therefore, low $\mu$. The arrow indicates a sample in which the $\nu = 5/2$ FQHS does not develop.

in Ref.[6], therefore, remains difficult to extract. Indeed, the dominance of the short-range scattering could not be ascertained and the gap altering effects of the combination of changing density and wavefunction confinement were not disentangled from that of the disorder [6]. In two other experiments, the effect on the $\nu = 5/2$ FQHS of a different type of disorder, that due to the remote ionized dopants was investigated [5, 7]. It was found that increasing the level of the remote dopants leads to the strengthening of the $\nu = 5/2$ FQHS [7]. A systematic dependence of the energy gap on overdoping, however, remains unavailable to date. Our results thus highlight the effect of the short-range alloy disorder on the stability of the $\nu = 5/2$ FQHS, whereas the effect of other important types of disorder, such as those of the long-range Coulomb potentials of dopants and of background impurities, remain unknown.

The lack of correlation of $\Delta_{5/2}$ and $\mu$ in alloy-free samples reported in the literature remains an outstanding puzzle [7, 16]. We propose that such a lack of correlation between $\Delta_{5/2}$ and $\mu$ appears because a) a well defined $\Delta_{5/2}$ versus $\mu$ correlation exists when only one type of disorder dominates and a single heterostructure design is employed and b) for each kind of disorder the $\Delta_{5/2}$ versus $\mu$ functional relationship is different. In other words, because high quality alloy-free samples most likely have a different mix of the various disorders and because $\Delta_{5/2}$ and $\mu$ track differently for each specific type of disorder, the result is a lack of correlation of $\Delta_{5/2}$ and $\mu$ when an analysis of dissimilar samples is undertaken. In contrast, when in a series of similar samples one type of disorder dominates, such as in our experiment, $\Delta_{5/2}$ and $\mu$ should be correlated. We suggest that the quasi-linear correlation of $\Delta_{5/2}$ and $\mu$ in our alloy samples shown in Fig.3 supports the above hypothesis. This hypothesis, however, remains to be tested in instances in which various other types of disorder are dominant. A natural consequence of our analysis is that $\mu$ measured at zero $B$-field, and the single-particle lifetime measured in the low $B$-field semi-classical regime [52] are poor measures of the impact of the disorder on many-body ground states developed at large $B$-fields [5–7, 47]. We note that we have measured the single-particle lifetime $\tau_q$ for our series of samples and found no obvious correlation with $\Delta_{5/2}$. The analysis of this data is left to a future publication.

As seen in the inset of Fig.2, above 100 mK there is little or no change with temperature in the magnetoresistance $R_{xx}$ at $\nu = 5/2$. According to the CF description, in this regime the system is described by a Fermi sea of the CFs in a zero effective magnetic field [53, 54]. We find the temperature-independent $R_{xx}$ value above 100 mK correlates with the amount of disorder. The values of $R_{5/2}^{150\mathrm{mK}}$, the saturation value of $R_{xx}$ at 150 mK measured at $\nu = 5/2$, are listed in the Supplementary Materials section. We notice that, $R_{5/2}^{150\mathrm{mK}}$ increases with an increasing $x$. According to the CF theory, $R_{5/2}^{150\mathrm{mK}}$ is a measure of the scattering of the CF with the impurities [53–56]. We conclude that the linear increase of $R_{5/2}^{150\mathrm{mK}}$ with $x$ is a direct consequence of enhanced scattering rate of the CFs as $x$ increases. We thus find that at $\nu = 5/2$ an increasing alloy disorder has two independent concurring effects: it reduces the energy gap of the state and it enhances $R_{5/2}^{150\mathrm{mK}}$, the $T$-independent $R_{xx}$ at $\nu = 5/2$ in the limit of high temperatures.

In an effort to speed up the screening of the samples and to characterize them at $^3$He refrigerator temperatures at which the $\nu = 5/2$ FQHS does not yet develop, it was proposed that strong $\nu = 5/2$ FQHSs develop in samples with low values of the $T$-independent $R_{xx}$ measured at $\nu = 5/2$ [47]. We thus found that such a hypothesis has a natural explanation within the framework of the composite fermion theory and, furthermore, that the hypothesis works in samples with alloy disorder. This hypothesis, however, remains to be further tested in samples with different types of dominating disorder.

We note that recently an alternative method of extracting the energy gap has been proposed [57]. This model, however, is formulated for the slowly varying potential generated by the remote dopants and it yet remains to be extended to alloy scattering. There is also effort in understanding short-range scatterers, albeit so far only for the $\nu = 1/3$ FQHS [58].

In conclusion, we have studied the effect of alloy disorder on the $\nu = 5/2$ FQHS in a regime in which alloy disorder dominates. The gap of the $\nu = 5/2$ FQHS closes at unprecedentedly low mobility which indicates that alloy disorder may not be as detrimental to the formation of the $\nu = 5/2$ FQHS as other types of disorder. Understanding disorder will lead to a better understanding of other parameters influencing the $\nu = 5/2$ FQHS, which will ultimately result in a better engineering of this state.

This work was supported by the DOE BES Experimental Condensed Matter Physics and Synthesis and Processing Science programs under the award No. desc0006671.

[1] P.W. Anderson, Phys. Rev. **109**, 1492 (1958).
[2] W. Li *et al.*, Phys. Rev. Lett. **94**, 206807 (2005); W. Li *et al.*, Phys. Rev. Lett. **102**, 216801 (2009).
[3] L.A. Wray *et al.*, Nature Physics. **7**, 32 (2011).
[4] J. Billy *et al.*, Nature Physics. **453**, 891 (2008); G. Roati *et al.*, Nature Physics. **453**, 895 (2008).
[5] V. Umansky *et al.*, J. Cryst. Growth. **311**, 1658 (2009).
[6] W. Pan *et al.*, Phys. Rev. Lett. **106**, 206806 (2011).
[7] G. Gamez and K. Muraki, Phys. Rev. B. **88**, 075308 (2013).
[8] B.E. Feldman, B. Krauss, J.H. Smet, and A. Yacoby, Science 337, 1196 (2012).
[9] A.P. Mackenzie *et al.*, Phys. Rev. Lett. **80**, 161 (1998).
[10] R.L. Willett *et al.*, Phys. Rev. Lett. **59**, 1776 (1987).

[11] W. Pan *et al.*, Phys. Rev. Lett. **83**, 3530 (1999).
[12] J.S. Xia *et al.*, Phys. Rev. Lett. **93**, 176809 (2004).
[13] J.P. Eisenstein, K.B. Cooper, L.N. Pfeiffer, and K.W. West, Phys. Rev. Lett. **88**, 076801 (2002).
[14] W. Pan *et al.*, Phys. Rev. B. **77**, 075307 (2008).
[15] H.C. Choi *et al.*, Phys. Rev. B. **77**, 081301 (2008).
[16] J. Nuebler *et al.*, Phys. Rev. B. **81**, 035316 (2010).
[17] A. Kumar *et al.*, Phys. Rev. Lett. **105**, 246808 (2010).
[18] Yang Liu *et al.*, Phys. Rev. Lett. **107**, 176805 (2011).
[19] C.R. Dean *et al.*, Phys. Rev. Lett. **100**, 146803 (2008).
[20] N. Samkharadze *et al.*, Phys. Rev. B. **84**, 121305 (2011).
[21] Guangtong Liu *et al.*, Phys. Rev. Lett. **108**, 196805 (2012).
[22] U. Wurstbauer, K.W. West, L.N. Pfeiffer, and A. Pinczuk, Phys. Rev. Lett. **110**, 026801 (2013)
[23] I.P. Radu *et al.*, Science. **320**, 899 (2008).
[24] M. Dolev *et al.*, Nature. **452**, 829 (2008).
[25] A. Bid *et al.*, Nature. **466**, 585 (2010).
[26] R.L. Willett, L.N. Pfeiffer, and K.W. West, Phys. Rev. B. **82**, 205301 (2010).
[27] V. Venkatachalam, A. Yacoby, L. Pfeiffer, and K. West, Nature **469**, 185 (2011).
[28] G. Moore and N. Read, Nucl. Phys. B. **360**, 362 (1991).
[29] M. Greiter, Xiao-Gang Wen, and F. Wilczek, Phys. Rev. Lett. **66**, 3205 (1991).
[30] P. Bonderson, V. Gurarie, and C. Nayak, Phys. Rev. B. **83**, 075303 (2011).
[31] C. Nayak, S.H. Simon, A. Stern, M. Freedman, and S. Das Sarma, Rev. Mod. Phys. **80**, 1083 (2008).
[32] V.W. Scarola, K. Park, and J.K. Jain, Nature **406**, 863 (2000).
[33] A.P. MacKenzie and Y. Maeno, Rev. Mod. Phys. **75**, 657 (2003).
[34] J. Sau, R.M. Lutchin, S. Tewari, and S. Das Sarma, Phys. Rev. Lett. **104**, 040502 (2010); J. Alicea, Phys. Rev. B **81**, 125318 (2010).
[35] A.J. Leggett, Rev. Mod. Phys. **47**, 331 (2003).
[36] A.C. Clark *et al.* , Rev. Sci. Instr. **81**, 103904 (2010).
[37] R.H. Morf, N. d'Ambrumenil, and S. Das Sarma, Phys. Rev. B. **66**, 075408 (2002).
[38] R. Morf and N. d'Ambrumenil, Phys. Rev. B. **68**, 113309 (2003).
[39] A. Wójs and J.J. Quinn, Phys. Rev. B 74, 235319 (2006).
[40] M.R. Peterson, Th. Jolicoeur, and S. Das Sarma, Phys. Rev. B 78, 155308 (2008).
[41] A.E. Feiguin, E. Rezayi, C. Nayak, and S. Das Sarma, Phys. Rev. Lett. 100, 166803 (2008).
[42] G.C. Gardner *et al.*, Appl. Phys. Lett. **102**, 252103 (2013).
[43] W. Li *et al.*, Appl. Phys. Lett. **83**, 2832 (2003).
[44] W. Li *et al.*, Phys. Rev. Lett. **105**, 076803 (2010).
[45] K.J. Friedland, R. Hey, H. Kostial, R. Klann, and K. Ploog, Phys. Rev. Lett. **77**, 4616 (1996).
[46] L.N. Pfeiffer, private communication
[47] M.J. Manfra, arXiv:1309.2717
[48] we used the software NextNano3, from the Walter Schottky Institute.
[49] Laroche at al, Appl. Phys. Lett. **96**, 162112 (2010).
[50] H.L. Stormer, D.C. Tsui, and A.C. Gossard, Rev. Mod. Phys. **71**, 298 (1999).
[51] N. Samkharadze *et al.*, Rev. Sci. Instrum. **82**, 053902 (2011).
[52] P.T. Coleridge, Phys. Rev. B **44**, 3793 (1991).
[53] J.K. Jain, Phys. Rev. Lett. **63**, 199 (1989).
[54] B.I. Halperin, P.A. Lee, and N. Read, Phys. Rev. B **47**, 7312 (1993).
[55] W. Kang *et al.*, Phys. Rev. Lett. **75**, 4106 (1995).
[56] J. Zhang, R.R. Du, J.A. Simmons, and J.L. Reno, Phys. Rev. B. **81**, 041308(R) (2010).
[57] N. d'Ambrumenil, B.I. Halperin, and R.H. Morf, Phys. Rev. Lett. **106**, 126804 (2011).
[58] D.N. Sheng *et al.*, Phys. Rev. Lett. **90**, 256802 (2003).

## SUPPLEMENTARY MATERIAL

We measured a series of quantum well samples with a different aluminum context $x$ in the electron channel. The width of the quantum well is 30 nm in each sample and certain relevant parameters are listed in Table.I. The capping GaAs layer is 10 nm thick, the electron gas is 200 nm deep under the sample surface, and the setback distance between the dopants and the quantum well is 75 nm on both sides of the well [1]. Further details pertaining to the growth procedure and characterization of our samples at 300 mK can be found in Ref.[1]. We note that the densities listed in Table.I may differ slightly from those listed in Ref.[1] because of slight variations due to thermal cycling.

It is instructive to compare the length scales associated with the alloy disorder we study. The average Al-Al distance within the electron channel of our samples ranges from 5.3-2.7 nm when $x$ is between 0.00057-0.0046. In comparison, the unintentionally added charged impurities during the MBE growth are estimated to have a concentration of about $10^{13}/\mathrm{cm}^3$, therefore their average separation is close to 0.5 $\mu$m [2, 3].

Each sample used in this study is a 4mm$\times$4mm square specimen. Eight indium-tin contacts are deposited on both the four corners and the middle points of the four edges of each specimen and are annealed in an forming gas atmosphere at 400 Celsius degrees for 10 minutes. A silver sinter heat exchanger is soldered onto each of the ohmic contacts using indium [5]. The sample and the silver heat exchangers are housed in a $He^3$ immersion cell. The role of this cell is to assure electron thermalization [4, 5] and to enable a magnetic field independent thermometry to these temperatures using a quartz $He^3$ viscometer [5].

The preparation of the electronic state is the same for each sample. Samples are cooled in our wet dilution refrigerator to about 5 K in the dark. Samples are then heated up to 10 K and are illuminated for 10 minutes with a red light emitting diode (LED). In order to maintain the same conditions for the LED illumination in different measurements, the LED is placed in a similar position with respect to each sample and the same bias current of 1 mA is used. After illumination, the sample is slowly cooled to 5 K over 2 hours, after which we proceed to condensing the $He^3$-$He^4$ mixture. Once most of the mixture is condensed, we start filling our $He^3$ immersion cell. We first obtained magnetotransport data, such as the ones shown in Fig.1 of the main text. A standard lock-in technique with a low excitation current of 2 nA at 11 Hz was used. The magnetoresistance measurements were followed by mobility measurements at zero magnetic field.

TABLE I. A summary of alloy content $x$, electron density $n(10^{11}/\mathrm{cm}^2)$, mobility $\mu(10^6\mathrm{cm}^2/\mathrm{Vs})$, scattering rate $1/\tau(1/\mathrm{ns})$, energy gap $\Delta_{5/2}(\mathrm{mK})$ of the $\nu = 5/2$ FQHS, and $R_{5/2}^{150\mathrm{mK}}(\Omega)$ of the measured samples.

| $x$ | $n$ | $\mu$ | $1/\tau$ | $\Delta_{5/2}$ | $R_{5/2}^{150\mathrm{mK}}$ |
|---|---|---|---|---|---|
| 0 | 3.08 | 20 | 1.3 | 569 | 27 |
| 0.00057 | 2.91 | 6.5 | 4.0 | 543 | 48 |
| 0.00075 | 2.88 | 5.0 | 5.2 | 360 | 83 |
| 0.0015 | 2.90 | 3.6 | 7.3 | 347 | 131 |
| 0.0026 | 2.70 | 2.7 | 9.7 | 199 | 209 |
| 0.0036 | 3.08 | 2.2 | 12 | 127 | 198 |
| 0.0046 | 2.82 | 1.7 | 15 | - | - |


[1] G.C. Gardner *et al.*, Appl. Phys. Lett. **102**, 252103 (2013).
[2] V. Umansky *et al.*, J. Cryst. Growth. **311**, 1658 (2009).
[3] M.J. Manfra, arXiv:1309.2717
[4] W. Pan *et al.*, Phys. Rev. Lett. **83**, 3530 (1999).
[5] N. Samkharadze *et al.*, Rev. Sci. Instrum. **82**, 053902 (2011).